The American Journal of Pathology, Vol. 180, No. 4, April 2012

DOI: 10.1016/j.ajpath.2011.12.033

Vascular Biology, Atherosclerosis, and Endothelium Biology

Endogenous Erythropoietin Protects Neuroretinal Function in Ischemic Retinopathy

Freya M. Mowat,* Francisco Gonzalez,*† Ulrich F.O. Luhmann,* Clemens A. Lange,*‡ Yanai Duran,* Alexander J. Smith,* Patrick H. Maxwell,§ Robin R. Ali,* and James W.B. Bainbridge*

From the Department of Genetics, University College London Institute of Ophthalmology, London, United Kingdom; the Department of Physiology,† School of Medicine, University of Santiago de Compostela, Santiago de Compostela, Spain; the University Eye Hospital,‡ Freiburg, Germany; and the Division of Medicine,§ University College London, London, United Kingdom*

Because retinal ischemia is a common cause of vision loss, we sought to determine the effects of ischemia on neuroretinal function and survival in murine oxygen-induced retinopathy (OIR) and to define the role of endogenous erythropoietin (EPO) in this model. OIR is a reproducible model of ischemia-induced retinal neovascularization; it is used commonly to develop antiangiogenic strategies. We investigated the effects of ischemia in murine OIR on retinal function and neurodegeneration by electroretinography and detailed morphology. OIR was associated with significant neuroretinal dysfunction, with reduced photopic and scotopic ERG responses and reduced b-wave/a-wave ratios consistent with specific inner-retinal dysfunction. OIR resulted in significantly increased apoptosis and atrophy of the inner retina in areas of ischemia. EPO deficiency in heterozygous Epo-Tag transgenic mice was associated with more profound retinal dysfunction after OIR, indicated by a significantly greater suppression of ERG amplitudes, but had no measurable effect on the extent of retinal ischemia, preretinal neovascularization, or neuroretinal degeneration in OIR. Systemic administration of recombinant EPO protected EPO-deficient mice against this additional suppression, but EPO supplementation in wild-type animals with OIR did not rescue neuroretinal dysfunction or degeneration. Murine OIR offers a valuable model of ischemic neuroretinal dysfunction and degeneration in which to investigate adaptive tissue responses and evaluate novel therapeutic approaches. Endogenous EPO can protect neuroretinal function in ischemic retinopathy. ***(Am J Pathol 2012, 180: 1726–1739; DOI: 10.1016/j.ajpath.2011.12.033)***

Retinal ischemia is a common feature of major causes of vision loss including diabetes,[1] retinal vascular occlusion,[2,3] and retinopathy of prematurity.[4] The retina has a uniquely high metabolic demand for oxygen that is normally met by a highly efficient vascular supply. Insufficiency of the retinal circulation causes neuroretinal dysfunction and degeneration. Focal retinal ischemia results in selective damage to specific subpopulations of retinal neurons and can result in cellular death by apoptosis or necrosis.[5] Dysfunction and degeneration of the inner retina in ischemic retinopathies leads directly to vision loss and is associated with characteristic changes in electroretinogram (ERG) responses.[6–8]

Endogenous adaptive responses can help protect against ischemic injury. In the eye, however, the associated angiogenic response is typically aberrant, causing severe vision loss through edema, hemorrhage, and fibrosis. Aberrant ischemia-induced angiogenesis exacerbates hypoxic neuroretinal injury and is the target of novel therapies, including inhibitors of vascular endothelial growth factor (VEGF). However, treatments with nonspecific angiostatic agents fail to take into account appropriate beneficial endogenous adaptive responses to hypoxia and so risk compromising critical neuroprotective

This work was supported by the Wellcome Trust (074617/Z/04/Z), the Medical Research Council (G03000341), the Newham Trust, Moorfields Eye Hospital Special Trustees, and the National Institute for Health Research Biomedical Research Centre for Ophthalmology at Moorfields Eye Hospital and the University College London Institute of Ophthalmology (J.W.B.B. and R.R.A.).

Accepted for publication December 8, 2011.

Portions of these data were presented at the annual meeting of the Association for Research in Vision and Ophthalmology (ARVO), May 2–6, 2010, in Fort Lauderdale, FL, and were published in abstract form (Invest Ophthalmol Vis Sci 2010;51:E-Abstract 4468).

Supplemental material for this article can be found at *http://ajp.amjpathol.org* or at doi: 10.1016/j.ajpath.2011.12.033.

Address reprint requests to James W.B. Bainbridge, Ph.D., Department of Genetics, UCL Institute of Ophthalmology, 11-43 Bath Street, London, UK. E-mail: j.bainbridge@ucl.ac.uk.

mechanisms. Therapeutic strategies can be made safer and more effective by considering how to protect and preserve these responses.

Ischemia-induced retinal dysfunction and degeneration are features of rodent models of retinal vascular occlusion[9,10] and diabetes.[11,12] However, the angiogenic response in these models is unpredictable. Oxygen-induced retinopathy (OIR) in the mouse is a reliable model of ischemia-induced retinal neovascularization[13] that has been used extensively in the investigation and preclinical development of novel antiangiogenic treatments such as inhibitors of VEGF[14–16] and erythropoietin (EPO).[17–19] However, the nature and extent of ischemic neurodegeneration and dysfunction has not been previously evaluated in murine OIR. Studies in the rat have demonstrated ischemia-induced retinal dysfunction after OIR that results in abnormal ERG a-wave, ERG b-wave, and oscillatory potentials (OPs).[8,20–22] The availability of transgenic strains, however, makes the mouse an attractive species to investigate disease mechanisms and to develop therapeutic strategies addressing ischemia-induced retinal neurodegeneration and neovascularization.

EPO is a widely distributed oxygen-regulated hormone and paracrine cytokine that acts on multiple pathways, including erythropoiesis, angiogenesis, and neuroprotection. Expression of *EPO* is predominantly in the kidney and liver postnatally,[23] but local expression is also evident in neuronal tissues, including the brain[24,25] and retina.[26,27] Specific disease processes may influence the location of EPO receptors in the retina.[28] Because EPO is proangiogenic and is expressed in the retina, it presents a potential target for antiangiogenic therapy in retinal neovascular disorders. Vitreous EPO levels are elevated in patients with ischemic retinal diseases, including retinal vascular occlusion,[29] diabetic retinopathy,[17,30,31] and retinopathy of prematurity.[32] In the hypoxic phase of murine OIR, retinal *EPO* expression is increased, and supplementation with high doses of EPO can be proangiogenic in this context.[33] Systemic EPO supplementation also has been shown to be an independent risk factor for the development of retinopathy of prematurity in premature babies.[34] Recent studies have advocated the use of EPO inhibitors such as *EPO*-targeting short interfering RNA (siRNA)[18] or antibodies[17] in the hypoxic phase of OIR, to inhibit neovascularization.

There is emerging evidence that proangiogenic factors such as VEGF and EPO have important roles in neuroprotection in the retina[35,36] and in the central nervous system.[37] Supplemental EPO can protect the adult retina from ischemic damage[38] and from light-induced retinal degeneration.[26,39] Many retinal neuronal cell types express receptors for EPO (EPO-R),[40,41] and EPO-R expression is up-regulated after retinal ischemia.[38] EPO may also have an important role in neurodevelopment in the eye and the brain.[24] Neurodevelopmental abnormalities in premature infants with systemic EPO deficiency[42] can be ameliorated by EPO supplementation.[43] To date, however, similar studies examining the effects of EPO on retinal neurodevelopment have not been performed.

The purpose of the present study was to determine the effect of ischemia on neuroretinal function and survival in murine OIR and to investigate the role of EPO in this model. We investigated the effect of ischemia in murine OIR on inner retinal function and neurodegeneration by electroretinography and detailed morphology, both in the short and long term. Using this model, we found that endogenous EPO can protect neuroretinal function.

Materials and Methods

Animals

The Epo-Tag transgenic mouse is described elsewhere.[44] Briefly, Epo-Tag mice have a 2.7-kb insertion of the viral simian virus 40 T (SV40T) antigen coding sequence into the 5′ untranslated region of the *Epo* gene.[44] This insertion leads to relative EPO deficiency, although homozygous mice do have a low level of EPO production from transcripts running through the viral polyA signal into the EPO coding sequence. Homozygous Epo-Tag$^{-/-}$ mice are profoundly anemic, whereas heterozygous Epo-Tag$^{+/-}$ adult mice are only mildly anemic.[45] We chose to evaluate heterozygous Epo-Tag mice in the present study, because the severe anemia in Epo-Tag$^{-/-}$ mice might influence OIR through an effect on oxygen delivery to the eye. Epo-Tag$^{+/-}$ mice were maintained on a C57Bl6J background (Harlan United Kingdom, Bicester, UK) as mixed litters of Epo-Tag$^{+/-}$ and wild-type animals (Epo-Tag$^{+/+}$). All animals were used with institutional ethical approval and under a United Kingdom Home Office project license and personal license. All procedures were performed in accordance with the Association for Research in Vision and Ophthalmology Statement for the Use of Animals in Ophthalmic and Vision Research.

Genotyping by PCR analysis was performed at postnatal day 7 (p7) and additionally after euthanasia. Ear-clip samples were digested using proteinase K (0.1 mg/mL in 30 mmol/L Tris-HCl pH 8.0 0.5% w/v SDS at 55°C for 16 hours; Sigma-Aldrich, Gillingham, UK), and genomic DNA was purified by ethanol. A commercial master mix containing Taq polymerase [1.1× ReddyMix PCR master mix and 1.5 mmol/L $MgCl_2$ (ABgene; Thermo Scientific, Epsom, UK)] was used according to the manufacturer's instructions. Primers used for genotyping mice were 5′-CGCACACACAGCTTCACCC-3′ (mEPO forward), 5′-CTGTAGGGCCAGATCACC-3′ (mEPO reverse), and 5′-GCCTAGGCCTCCAAAAAAGC-3′ (SV40T reverse). Separate reactions were performed on each ear-clip sample to determine the presence of the wild-type mEPO allele and the SV40T allele.

The Mouse Model of Oxygen-Induced Retinopathy

Nursing mothers and their pups were placed in a 75% oxygen supply chamber from p7 to p12, as described previously.[13] A constant low flow of 80% oxygen (with the balance as nitrogen) was provided to a closed acrylic glass chamber. The oxygen level was monitored twice daily, and maintained at 75% ± 3% O_2. The mice were

exposed to a standard 12-hour light-dark cycle. Samples were collected at various time points after the return to room air.

Measurement of Hematocrit

Hematocrit measurement was performed as a terminal procedure, because of the limited blood volume in young mice and the potential for induced anemia from repeated blood sampling. Animals were terminally anesthetized, and venous blood was obtained from the right atrium immediately after death. Blood was collected directly into heparinized microhematocrit capillary tubes (Hawksley; Lancing, UK), to prevent clotting. Samples were spun at 5,400 $\times$ *g* for 5 minutes in a microhematocrit centrifuge (Biodynamics Selectafuge 24; BCL, Lewes, UK), and the percentage packed cell volume (%PCV) was calculated using a premeasured scale.

Supplementation with Recombinant Human EPO

Supplementation with recombinant human erythropoietin (rHuEPO) (Epoetin alfa, 40,000 U/mL; Janssen-Cilag, High Wycombe, UK) was administered systemically by intraperitoneal injection starting at p14 and ending at p25 at a dose rate of 5000 U/kg diluted in PBS, as described previously.[26,33] Each animal was weighed daily, and dosing was administered per 0.1 g body weight in a maximum volume of 0.15 mL. Previous studies have shown that systemic supplementation with erythropoietin in murine OIR from p14 to p16 does not affect the vascular phenotype at p17.[33]

Electroretinography

Mice were anesthetized using an intraperitoneal injection of a mixture containing medetomidine hydrochloride (1 mg/mL Domitor; Pfizer Animal Health, Kent, UK), ketamine (100 mg/mL; Fort Dodge Animal Health, Southampton, UK), and sterile water in the ratio 5:3:42. Anesthesia was reversed using an intraperitoneal injection of the reversal agent atipamezole hydrochloride (Antisedan, 5 mg/mL; Pfizer Animal Health) in sterile water (ratio 1:50). Electroretinography (ERG) was performed at p26 and p60. Mice were dark-adapted for 16 hours. Animals were anesthetized for ERG, and pupils were dilated using 1% tropicamide (Minims; Bausch & Lomb, Kingston-on-Thames, UK) applied topically. Water-based ocular lubricant (Viscotears; Novartis Pharmaceuticals United Kingdom, Camberley, UK) was used to improve electrical contact with the electrode and to keep the eyes moist during the procedure. All manipulations before scotopic ERG were performed under dim red-light illumination. ERGs were obtained using an Espion ERG system (Diagnosys, Cambridge, UK). Ganzfeld ERGs were obtained from both eyes simultaneously using contact platinum corneal electrodes on each eye; one reference electrode was placed sublingually, and the ground electrode was placed subdermally in the midline at the base of the tail. Electrical impedance was balanced for each eye before recording ($\sim$10 kΩ). A scotopic flash intensity series was performed, followed by light-adapted photopic flicker measurements. In all measurements, 400 ms of response was recorded. Recordings were filtered from 0 to 1 kHz and were digitized with a sampling frequency of 5 kHz. The first 10 ms before the stimulus onset of each recording was automatically used to set zero for the trace.

For scotopic flash examination, a multiple white-light flash intensity series was performed, with light intensity increasing in six steps from 0.001 cd $\cdot$ s/m^2 to 5 cd $\cdot$ s/m^2. Ten responses (for intensities $<$1 cd $\cdot$ s/m^2) or five responses (for intensities $\geq$1 cd $\cdot$ s/m^2) per intensity were collected and averaged for use in subsequent analysis. Measurements for amplitude and implicit time were taken from the trough of the a-wave to the peak of the b-wave. The photopic a-wave was defined as the maximal negative amplitude after the onset of light exposure. The photopic b-wave was defined as the maximal positive amplitude after the onset of light exposure, compensating visually for the waveforms of the OPs. Statistical comparison was performed at the 1 cd $\cdot$ s/m^2 intensity representing a mixed rod-cone response[46] and provided the maximal a-wave amplitude. OPs were obtained with a fifth-order Butterworth filter and 65- to 235-Hz bandpass using a custom-made program coded in MATLAB (MathWorks, Natick, MA), as described previously.[8,46] OP 1 was not analyzed, because of the potential for a-wave contamination. Analysis of OPs was performed to determine the sum of the OP amplitudes of OP 2 to 5 (SOPA).[8] The OPs were also analyzed in the frequency domain by using a fast Fourier transformation with the first 128 ms of each recording, previously filtered with a fifth-order Butterworth filter as detailed previously. This produced a power spectrum distribution that was calibrated as described previously.[8] The resulting calibrated data were fit by a Gaussian curve; the area under the curve was calculated and used to quantify OP energy, as described previously.[8]

Photopic flicker examination was performed on light-adapted (10 minutes light adaptation time, 10 cd/m^2 intensity) mice after scotopic recording. A photopic flicker frequency series (from 0.5 to 15 Hz) was performed with a standard bright white light (3 cd $\cdot$ s/m^2 with a background intensity of 10 cd/m^2). Analysis was performed on the average recording made from 25 recordings per frequency. Analysis of cone flicker amplitude and implicit time was performed on photopic flicker ERGs at the 10-Hz frequency, because according to previous report this is the maximal amplitude in the mouse flicker ERG.[47] Amplitudes were measured from the trough of the a-wave to the peak of the b-wave, and an average of three measurements was used in subsequent analysis.

Histology and Immunohistochemistry

For lectin staining of retinal vasculature in retinal flatmounts, eyes were fixed in 4% paraformaldehyde for 1 hour, and the lens and cornea were removed. Eyecups were washed and then incubated with 0.1 mg/mL tetramethylrhodamine isothiocyanate-conjugated *Bandeiraea*

simplicifolia lectin (Sigma-Aldrich) in PBS overnight at 4°C. Retinas were dissected from the eyecup, radial cuts were made to flatten the retina, and the retinas were mounted with fluorescent aqueous mounting medium (Dako, Ely, UK), ganglion cell layer uppermost, using a coverslip. Lectin-stained retinal flatmounts from p12 and p17 mice from the OIR model were assessed as described previously.[48,49] Retinas were imaged using a Zeiss LSM 510 confocal microscope at 5× magnification (Carl Zeiss Microimaging, Göttingen, Germany). A single x/y plane was taken from each quadrant of the retina and the central retina at 1024 × 1024 pixel resolution. Composite images were constructed using Photoshop CS2 software (Adobe Systems, Uxbridge, UK). Images were loaded into an image analysis program (Image Pro Plus; Media Cybernetics, Bethesda, MD) and converted to 16-bit grayscale images. The total vascularized retina and the capillary-free area were delineated and the areas were calculated. Areas of neovascularization were outlined, and the manual selection tool was used to highlight the bright neovascular areas only. The neovascular and ischemic areas were represented as percentages of total retinal area; these values were used in subsequent analysis.

The TUNEL procedure for detection of DNA fragmentation (a marker of apoptosis) was performed using a commercial kit according to the manufacturer's instructions (Chemicon ApopTag Red *in situ* apoptosis detection kit; Millipore, Livingston, UK). For quantification of apoptotic nuclei, the number of apoptotic cells was counted in each retinal layer in three 12-μm central retinal cryosections, 60 μm apart. An average value per eye (and per animal, if both eyes were examined) was calculated and used in subsequent analysis.

For pimonidazole immunohistochemistry, 60 mg/kg pimonidazole hydrochloride (Chemicon Hypoxyprobe-1; Millipore) diluted in sterile PBS was administered by intraperitoneal injection 3 hours before euthanasia, as described previously.[48,50] Animals were euthanized and eyes were fixed by perfusion with 4% paraformaldehyde. Retinal cryosections were incubated with fluorescein isothiocyanate-conjugated anti-pimonidazole antibody [Chemicon (Millipore)] at a dilution of 1:50 for 1 hour at room temperature.

Collagen IV immunostaining of retinal vasculature was performed on retinal cryosections. Anti-collagen IV antibody (AbD Serotec, Oxford, UK) was incubated at a dilution of 1:300 for 16 hours at 4°C, followed by anti-rabbit secondary antibody (goat anti-rabbit Alexa Fluor 594; Invitrogen Molecular Probes, Paisley, UK) incubated at room temperature for 1 hour at a dilution of 1:200.

For analysis of retinal thickness, enucleated eyes were fixed in Serra's fixative [60% (v/v) ethanol, 30% (v/v) saturated formaldehyde, 10% (v/v) concentrated acetic acid] at 4°C for 16 hours and then were embedded in paraffin using an automated tissue-processing system (TP1020; Leica Microsystems, Wetzlar, Germany). Sections 6 μm thick were stained with H&E, and three central sagittal retinal sections per eye were selected that transected the optic nerve. Sections were photographed using a light microscope (Leitz Diaplan microscope; Leica Microsystems) equipped with a QImaging MicroPublisher 5.0 digital camera and QCapture Pro software version 6.0 (QImaging, Surrey, BC, Canada) at ×40 magnification. A calibration slide with 10-μm gradations was imaged at the same resolution, to facilitate measurement. Measurements were taken at 150-μm intervals either side of the optic nerve head toward the periphery. Measurement was performed using commercial image analysis software (Image-Pro Plus version 5.1; Media Cybernetics, Bethesda, MD). For each region, the total retinal thickness from the edge of the nerve fiber layer to the outer edge of the outer nuclear layer was measured. Individual measurements were made for the nerve fiber layer, inner plexiform layer, inner nuclear layer, outer plexiform layer, and outer nuclear layer.

Real-Time RT-PCR

RNA was extracted from mouse retinal tissue ($n = 3$ eyes per group) using a commercial kit (RNeasy mini kit; Qiagen, Crawley, UK). The amount of template RNA was measured using a small-volume spectrophotometer (NanoDrop ND-1000; Thermo Scientific, Wilmington, DE). Equal amounts of RNA were used for all samples as a template for cDNA manufacture. cDNA was made from template RNA using a commercial kit (QuantiTect Reverse Transcriptase Kit; Qiagen). Real-time quantitative RT-PCR was performed using an ABI 7900HT thermal cycler with its associated software, SDS version 2.2.2 (Applied Biosystems, Foster City, CA). The 5′ nuclease technique based on Taq polymerase and FAM labeled hydrolysis probes was used for all real-time reactions, using commercially designed primer/probe combinations (Roche Universal Probe Library; Roche Diagnostics, Burgess Hill, UK). The mEPO primers were 5′-TCTGCGACAGTCGAGTTCTG-3′ (forward) and 5′-CTTCTGCACAACCCATCGT-3′ (reverse); the probe sequence used was 5′-GGAGGCAG-3′ (probe #16; Roche Diagnostics). The EPO real-time assay was designed to detect both wild-type EPO and Epo-Tag RNA. All reactions were performed in triplicate. For all test samples, the endogenous control β-actin was used to verify equal loading and to facilitate relative quantitation calculation. The mβ-actin primers were 5′-AAGGCCAACCGTGAAAAGAT-3′ (forward) and 5′-GTGGTACGACCAGAGGCATAC-3′ (reverse); the probe sequence was 5′-TGCTGTCC-3′ (probe #56; Roche Diagnostics). The $\Delta\Delta C_T$ method of relative quantitation was used to compare data.

ELISA

After terminal anesthesia, mice were perfused with 20 mL of PBS to remove residual blood from the vasculature. Whole eyes were snap-frozen in liquid nitrogen. Eyes were homogenized in sterile PBS with protease inhibitors (Sigma-Aldrich) using a plastic homogenizer. The homogenate was spun at 2800 × *g* for 10 minutes. Protein concentration of the supernatant was determined using a colorimetric protein assay performed in triplicate (DC protein assay kit; Bio-Rad Laboratories, Hemel Hempstead, UK) and compared with a bovine serum albumin standard curve. Sample endpoint enzyme-linked immu-

nosorbent assay (ELISA) was measured in triplicate using an EMax microplate reader (Molecular Devices, Berkshire, UK), comparing the optical density at 450 nm with a reference at 650 nm. The quantity of murine erythropoietin (mouse erythropoietin Quantikine ELISA development kit; R&D Systems, Minneapolis, MN) or human erythropoietin (human erythropoietin Quantikine ELISA development kit; R&D Systems) was calculated per milligram of whole-eye protein, comparing each sample to a bovine serum albumin (10 mg/mL; New England Biotechnology, Hitchin, UK) standard curve of known concentration.

Statistical Analysis

For data obtained from both eyes, the mean value per animal was calculated and used in subsequent analysis. Unpaired Student's *t*-tests were used when two unmatched groups were compared. One-way analysis of variance was used to compare three unmatched groups. Two-way analysis of variance was used when comparisons were made with two or more interconnected variables (eg, oxygen treatment and genotype). The Bonferroni post hoc test was used to examine differences further. For data presented in figures, the statistical test used is specified along with the *P* values. A *P* value of <0.05 was considered significant. Statistical analysis was performed using a commercial program (GraphPad Prism version 5.00 for Windows, San Diego, CA). Data in graphs are expressed as means ± SEM.

Results

EPO Expression Is Up-Regulated in the Eye and the Kidney during OIR

In OIR, exposure of mouse pups to a hyperoxic environment (75% oxygen) from p7 to p12 results in capillary ablation in areas of the central retina. On return to room air at p12, these areas of retinal ischemia become hypoxic, and the associated up-regulation of proangiogenic cytokines leads to aberrant, preretinal neovascularization.[13,50] To investigate the effect of hypoxia in OIR on expression of *EPO*, we used real-time RT-PCR to measure *EPO* mRNA in the eyes of Epo-Tag$^{+/+}$ and Epo-Tag$^{+/-}$ littermates with OIR at p13 and in control animals raised in normoxia throughout. To identify any effect on systemic expression of EPO, we also measured renal *EPO* mRNA. The return to room air from hyperoxia was associated with up-regulated expression of *EPO* at p13 in both eyes and kidneys of both Epo-Tag$^{+/+}$ and Epo-Tag$^{+/-}$ animals (Figure 1A). This finding suggests that hypoxia in this model is not limited to the retina and has potentially relevant systemic effects. The up-regulated expression of *EPO* in OIR was significantly less marked in the eyes and kidneys of Epo-Tag$^{+/-}$ animals than in those of Epo-Tag$^{+/+}$ littermates (Figure 1A), confirming that these mice have a blunted *EPO* response to hypoxia.

To evaluate the effect of *EPO* up-regulation on ocular EPO protein concentration, we also examined whole eyes for EPO protein by ELISA ($n = 8$ independent eyes per group). The concentration of EPO in eyes of Epo-Tag$^{+/+}$ mice at p13 was significantly higher in OIR than in control animals raised in normoxia throughout (Figure 1B). The concentration of EPO in eyes of Epo-Tag$^{+/-}$ mice after OIR at p13 was significantly lower than in Epo-Tag$^{+/+}$ littermates. These findings confirm that the lack of significant *EPO* up-regulation in response to hypoxia in Epo-Tag$^{+/-}$ mice is associated with a deficiency of intraocular EPO.

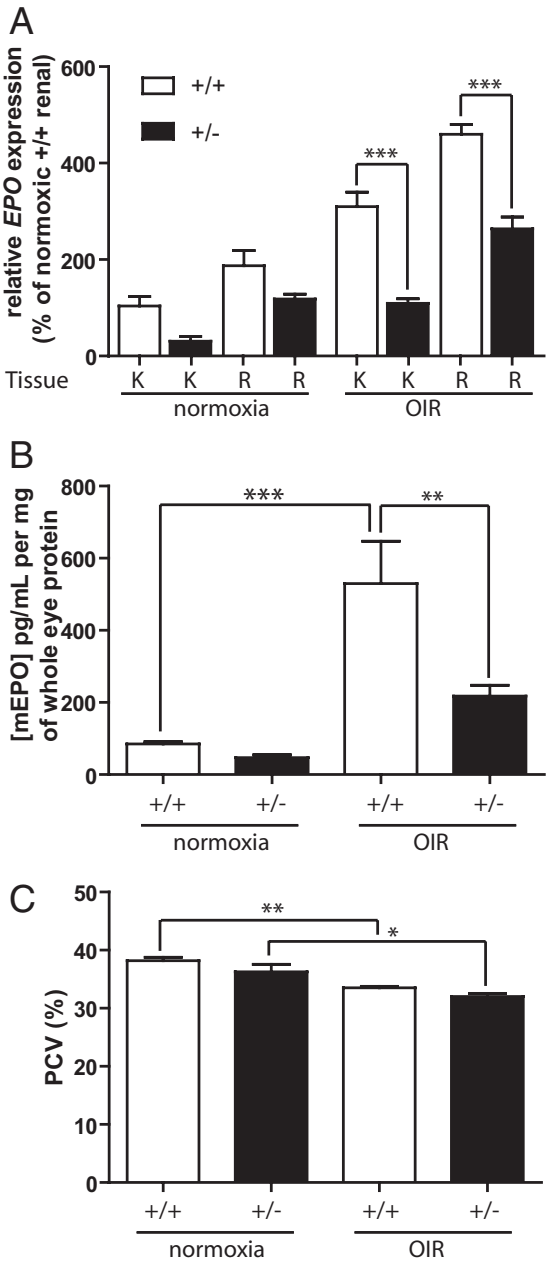

Figure 1. OIR is associated with up-regulation of EPO mRNA and protein in the kidney and the retina. **A:** At p13, both renal and retinal *EPO* mRNA were up-regulated after OIR in both Epo-Tag$^{+/+}$ and Epo-Tag$^{+/-}$ mice, but Epo-Tag$^{+/+}$ mice had significantly greater up-regulation in OIR than Epo-Tag$^{+/-}$ mice ($n = 3$ per group). **B:** Epo-Tag$^{+/-}$ mice also had a blunted EPO protein presence after OIR in contrast to Epo-Tag$^{+/+}$ mice as shown by whole-eye EPO protein ELISA at p13 ($n = 8$ per group). **C:** A mild but significant reduction in hematocrit (%PCV) was observed in both Epo-Tag$^{+/+}$ and Epo-Tag$^{+/-}$ mice after OIR at p13 ($n = 4$ per group). $^{*}P < 0.05$, $^{**}P < 0.01$, and $^{***}P < 0.001$ two-way analysis of variance with Bonferroni correction for multiple analyses. K, kidney; R, retina.

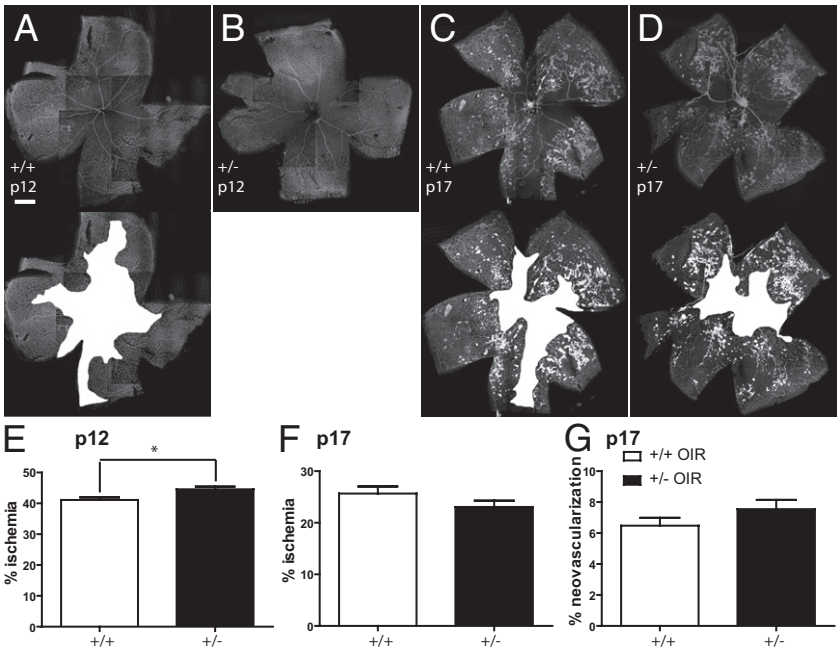

Figure 2. OIR-induced ischemia and neovascularization is minimally affected in Epo-Tag$^{+/-}$ animals. The mice were subjected to OIR from p7 to p12. **A** to **D:** Representative retinal flatmounts are shown for p12 and p17. **A:** Epo-Tag$^{+/+}$ (n = 8). **B**: Epo-Tag$^{+/-}$ (n = 8). **C**: Epo-Tag$^{+/+}$ (n = 10). **D**: Epo-Tag$^{+/-}$ n = 11). **Upper** images show staining for vasculature (tetramethylrhodamine isothiocyanate-conjugated *B. simplicifolia* lectin); **lower** images show the corresponding areas of ischemia (central filled area) and neovascularization (diffuse white areas highlighted within vascularized retinal area). Scale bar = 500 μm. **E** to **G:** Quantification of ischemia at p12 was slightly higher in Epo-Tag$^{+/-}$ mice (**E**), but by p17 neither ischemia (**F**) nor neovascularization (**G**) were significantly different compared with wild-type littermates. *$P < 0.05$ unpaired t-test.

To investigate whether oxygen delivery to the eye might be compromised in Epo-Tag$^{+/-}$ mice, we measured the hematocrit (%PCV) in animals at p13. The hematocrit was lower in mice with OIR (33.5 ± 0.3% for Epo-Tag$^{+/+}$ versus 32 ± 0.6% for Epo-Tag$^{+/-}$; n = 4 per group) than in normoxic controls (38.2 ± 0.6% for Epo-Tag$^{+/+}$ versus 36.3 ± 1.3% for Epo-Tag$^{+/-}$; n = 4 per group), but we detected no significant difference in hematocrit between Epo-Tag$^{+/-}$ and Epo-Tag$^{+/+}$ littermates (Figure 1C).

Body weight at p13 did not differ between Epo-Tag$^{+/-}$ and Epo-Tag$^{+/+}$ in normoxia or after OIR (data not shown). Wild-type animals were significantly smaller at p13 in OIR, compared with normoxic controls (5.7 ± 0.05 g OIR versus 7.3 ± 0.3 g normoxic, $P < 0.05$).

EPO Deficiency in Epo-Tag$^{+/-}$ Mice Does Not Attenuate Ischemia-Induced Retinal Neovascularization in OIR

To investigate the effect of EPO deficiency on ischemia-induced retinal neovascularization, we examined *B. simplicifolia* lectin-stained retinal flatmounts of Epo-Tag$^{+/-}$ mice with OIR. To identify the effect of hyperoxia on capillary ablation, we measured the ischemic area in retinal flatmounts at p12 after OIR (n = 8 independent eyes per group); representative flatmounts are shown in Figure 2, A and B. To investigate the effect on neovascularization, we measured the ischemic and neovascular areas at p17; representative flatmounts are shown in Figure 2, C and D. Epo-Tag$^{+/-}$ mice developed a marginally greater (3.5% greater) area of retinal capillary ablation at p12, compared with Epo-Tag$^{+/+}$ littermates (Figure 2E). At p17, however, there were no significant differences between genotype in retinal ischemic area or neovascular area (Figure 2, F and G; n = 10 independent eyes for Epo-Tag$^{+/+}$ and n = 11 independent eyes for Epo-Tag$^{+/-}$). These data suggest that relative EPO deficiency in Epo-Tag$^{+/-}$ mice during the hyperoxic phase of OIR may contribute marginally to additional capillary ablation, as has been previously demonstrated,[33] but that this relative deficiency of endogenous EPO in the hypoxic phase of OIR does not prevent the typical aberrant retinal neovascular response to hypoxia in this model.

OIR Is Associated with Substantial Inner Retinal Apoptosis in Areas of Ischemia/Hypoxia and Mild Apoptosis throughout the Outer Retina

To define the influence of ischemia/hypoxia on neuroretinal degeneration in OIR, we investigated apoptosis by TUNEL staining of retinal cryosections at time points during OIR development. At p13, apoptosis in both the inner and outer nuclear layers was increased in animals with OIR, compared with those raised in normoxia throughout (Figure 3).

The density of inner nuclear layer apoptotic cells correlated closely with the area of capillary ablation and hypoxia, as demonstrated by the absence of collagen IV-stained vasculature and the strength of pimonidazole binding (Figure 3, A and B). Greater numbers of TUNEL-stained cells were evident in the inner nuclear layer of both Epo-Tag$^{+/+}$ and Epo-Tag$^{+/-}$ animals at p13 in OIR, compared with control animals raised in normoxia throughout (n = 8 per group; Figure 3C).

Apoptotic cells in the outer nuclear layer at p13 were distributed across the retina and were not restricted to areas of inner retinal ischemia/hypoxia. Greater numbers of TUNEL-stained cells were evident in the outer nuclear layer of both Epo-Tag$^{+/+}$ and Epo-Tag$^{+/-}$ animals at p13 in OIR, compared with control animals raised in normoxia throughout (n = 8 per group; Figure 3D). The increase in

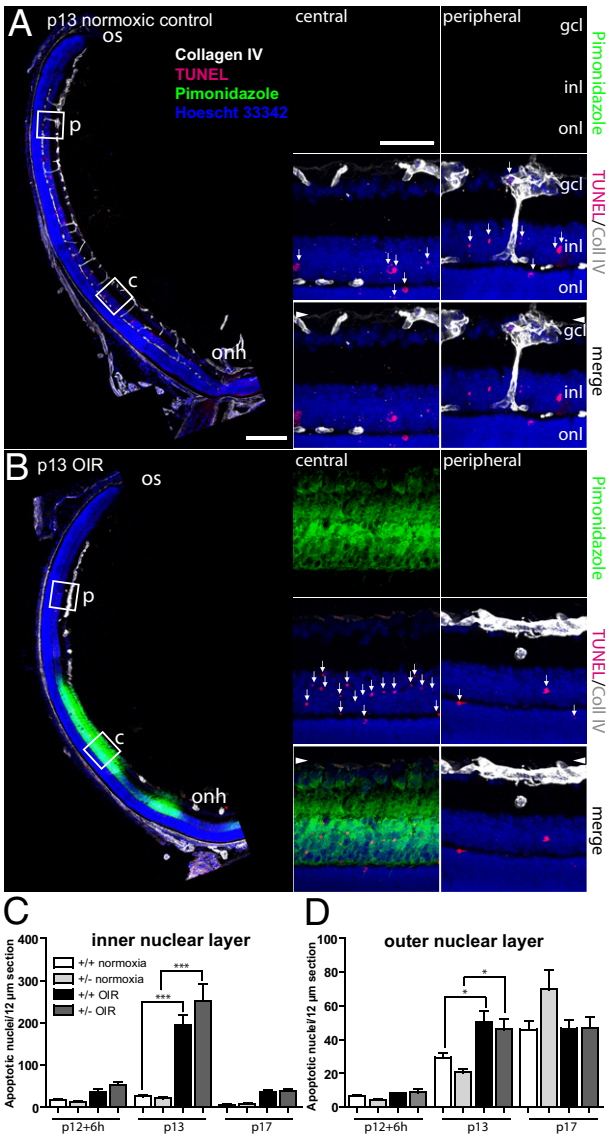

Figure 3. Hypoxia in OIR is associated with retinal apoptosis. Retinas from Epo-Tag$^{+/+}$ mice raised in normoxia (**A**) and OIR 24 hours (**B**) after return to room air at p13 were evaluated to determine the extent and distribution of apoptosis. Immunohistochemistry was performed for apoptotic nuclei (TUNEL; red), hypoxic protein (pimonidazole; green), and retinal vasculature (collagen IV; white). Staining was performed on 12-μm frozen retinal sections. **Boxed** regions at the **left** are shown at higher magnification at the **right** (c, central; p, peripheral). **Arrows** indicate apoptotic cells; an **arrowhead** in the **bottom panels** indicates the position of the inner limiting membrane. **C** and **D**: Apoptosis at p12 + 6 hours, p13 and p17 was quantified in all retinal layers in both Epo-Tag$^{+/+}$ and Epo-Tag$^{+/-}$ mice (n = 8 per group). OIR at p13 was associated with a significant increase in apoptosis in the inner retina (**C**) and outer retina (**D**) in both Epo-Tag$^{+/-}$ and Epo-Tag$^{+/+}$ mice. gcl, ganglion cell layer; inl, inner nuclear layer; onh, optic nerve head; onl, outer nuclear layer; os, ora serrata. $^{*}P < 0.05$, $^{***}P < 0.001$ two-way analysis of variance with Bonferroni post hoc test. Scale bars: 250 μm (**A** and **B**, **left**); 50 μm (**A** and **B**, **right**).

apoptosis at this time point represented a very small proportion of the outer nuclear layer cells, and no difference was detected at the p17 time point.

We detected no difference in the number of apoptotic cells between Epo-Tag$^{+/-}$ and Epo-Tag$^{+/+}$ littermates at p12 + 6 hours, at p13, or at p17 (n = 3 per group; Figure 3, C and D). Apoptosis in the retinal pigment epithelium and ganglion cell layer was unaffected by OIR in Epo-Tag$^{+/-}$ and Epo-Tag$^{+/+}$ animals, and we identified no difference in the number of apoptotic cells between Epo-Tag$^{+/-}$ and Epo-Tag$^{+/+}$ wild-type mice (data not shown).

Inner Retinal Ischemia/Hypoxia Results In Focal Retinal Degeneration and Sustained Activation of Retinal Müller Glia

To evaluate the long-term consequences of local retinal ischemia/hypoxia on retinal morphology, we examined retinas from animals at p60. To determine the effect of ischemia/hypoxia in OIR on the thickness of the retinal layers, we examined paraffin-embedded retinal sections from Epo-Tag$^{+/+}$ mice and Epo-Tag$^{+/-}$ littermates that had been raised in normoxia or undergone OIR (n = 5 or 6 animals per group). OIR induced considerable thinning of the central retina, in a configuration that correlates closely with the area of ischemia/hypoxia in this model. Total retinal thickness was substantially less in animals with OIR than in normoxic controls (Figure 4A). Significant thinning was detected in the nerve fiber layer (Figure 4B), inner plexiform layer (Figure 4C), inner nuclear layer (Figure 4D), and outer plexiform layer (Figure 4E). We measured no effect of OIR on thickness of the outer nuclear layer (Figure 4F). We detected no differences in thickness of retinal layers between Epo-Tag$^{+/-}$ and wild-type littermates in any region of the retina in OIR or in control animals raised in normoxia. Representative images are shown from retinas of a normoxic Epo-Tag$^{+/+}$ animal in Figure 4G and from an Epo-Tag$^{+/+}$ mouse with OIR in Figure 4H.

To investigate the effect of OIR on activation of retinal glia, we performed immunohistochemistry for glial fibrillar acidic protein in animals at p60 (GFAP) (n = 4 animals per group). All glial cells were labeled using vimentin. In retinas of wild-type animals raised in normoxia, GFAP labeled only astrocytes, with very few glial cells labeled throughout the retina, except at the retinal periphery (Figure 4, I and J). In contrast, in retinas of animals with OIR, we found the majority of glial cells to be activated, with GFAP-positive cells throughout the retina (Figure 4, K and L). Up-regulation of GFAP in glia was detected at p17 in the central retina, and at p26 extending beyond presumed areas of hypoxia (see Supplemental Figure S1 at *http://ajp.amjpathol.org*). We detected no differences in glial activation between Epo-Tag$^{+/-}$ and Epo-Tag$^{+/+}$ wild-type animals.

OIR Results in Sustained Dysfunction of the Inner Neuroretina, and EPO-Deficient Epo-Tag$^{+/-}$ Mice Also Develop Dysfunction of the Outer Neuroretina

To determine the effect of OIR on neuroretinal function, we performed scotopic (dark-adapted, rod-mediated) and photopic (light-adapted, cone-mediated) ERGs in Epo-Tag$^{+/+}$ mice and Epo-Tag$^{+/-}$ littermates (n = 4 to 9 animals per group). Representative ERG waveforms are

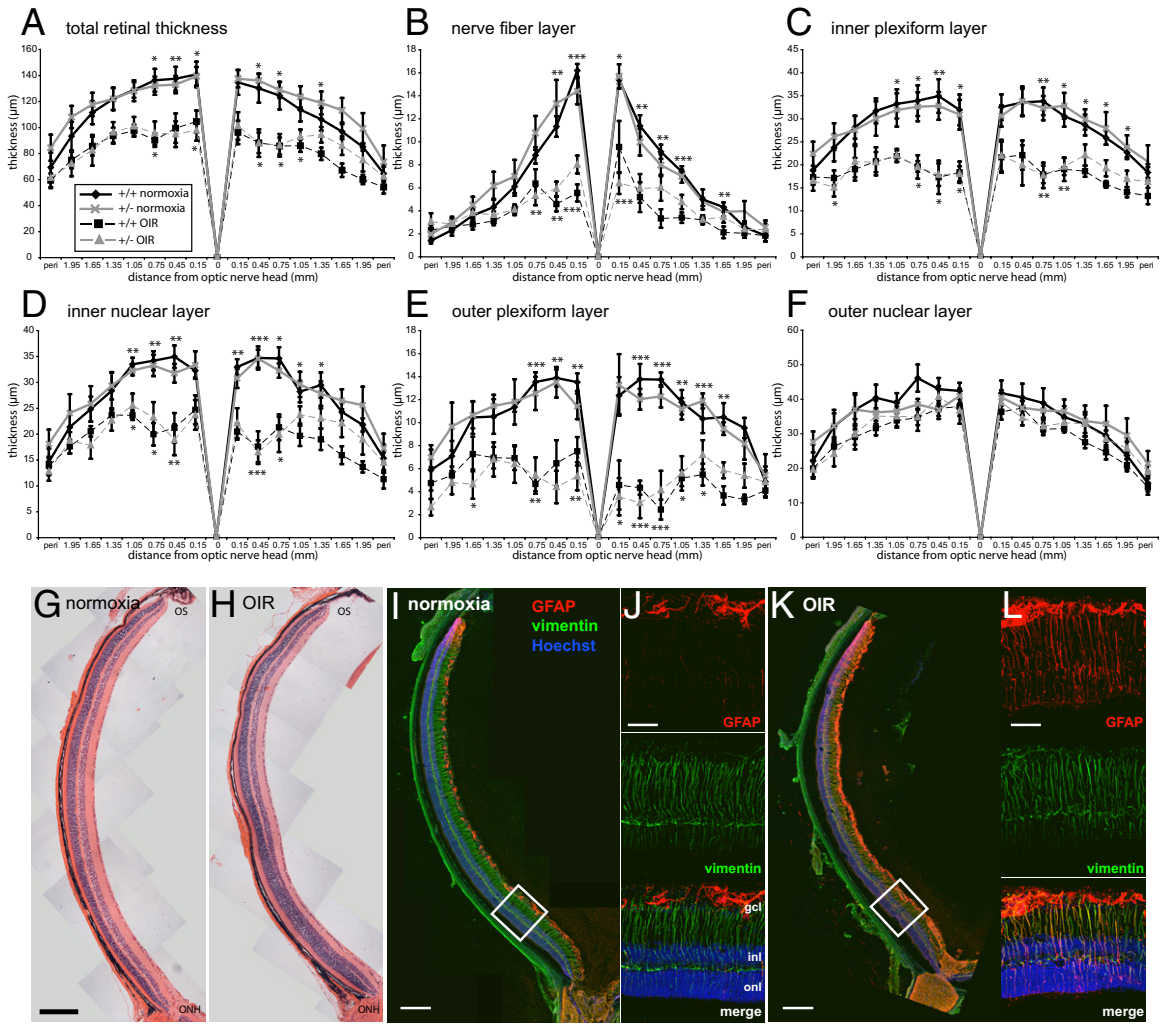

Figure 4. OIR is associated with retinal thinning and sustained glial stress. Measurement of retinal thicknesses at p60 after normoxia or OIR showed that OIR was related to significant thinning of the central retina (**A**) and comprised thinning of the nerve fiber layer (**B**), inner plexiform layer (**C**), inner nuclear layer (**D**), and outer plexiform layer (**E**). Outer nuclear layer thickness was unaffected by OIR (**F**). There were no differences between Epo-Tag$^{+/+}$ and Epo-Tag$^{+/-}$ mice in any measured parameter. $^{*}P < 0.05$, $^{**}P < 0.01$, and $^{***}P < 0.001$ two-way analysis of variance with Bonferroni post hoc test. *P* values are given for the comparison between normoxia and hypoxia, with Epo-Tag$^{+/+}$ *P* values shown above the line graphs and Epo-Tag$^{+/-}$ *P* values below the line graphs. **G** and **H:** Representative images of H&E-stained retinas from animals at p60 that had been reared in normoxia (**G**) and OIR (**H**). Original magnification, ×20. **I** to **K**: Representative images of retinal cryosections stained using antibodies targeting GFAP (red) and vimentin (green) from animals at p60 reared in normoxia (**I**) and OIR (**K**), with **boxed** areas shown in higher magnification at the **right** (**J** and **L**, respectively). Original magnification: ×20 (**I** and **K**); ×40 (**J** and **L**). gcl, ganglion cell layer; heterozygous (Epo-Tag$^{+/-}$); inl, inner nuclear layer; ONH, optic nerve head; onl, outer nuclear layer; OS, ora serrata; peri, peripheral retina; wt, wild type (Epo-Tag$^{+/+}$).

shown from Epo-Tag$^{+/+}$ mice at p26 (Figure 5A) and p60 (Figure 5B). After OIR, Scotopic ERG a-wave and b-wave amplitudes at p26 and p60 were significantly reduced in Epo-Tag$^{+/+}$ and Epo-Tag$^{+/-}$ animals, compared with Epo-Tag$^{+/+}$ or Epo-Tag$^{+/-}$ animals raised in normoxia (Figure 5, C and D). There was no difference in body weight between any groups at p26 (data not shown). Epo-Tag$^{+/-}$ mice with OIR had significantly lower a-wave and b-wave amplitudes at both p26 and p60, compared with Epo-Tag$^{+/+}$ littermates with OIR, indicating inhibition of both inner and outer retinal function (Figure 5, C and D). The reduction in b/a wave ratio after OIR at p26 and p60 was proportional in both genotypes (Figure 5E), which is consistent with a preferential and sustained dysfunction of the inner retina, a characteristic of severe ischemic retinopathies in humans.[51] In comparison with Epo-Tag$^{+/+}$ mice, Epo-Tag$^{+/-}$ mice had additional reductions in a-wave amplitude (Figure 5C), with corresponding b-wave amplitude reductions (Figure 5D). This finding indicates that EPO deficiency might contribute to additional outer neuroretina dysfunction after OIR.

Analysis of OPs from scotopic ERGs demonstrated that the sum of the peak OP amplitude of OPs 2 to 5 (Figure 5F) and OP energy (Figure 5G) at p26 and p60 were significantly reduced by OIR in both Epo-Tag$^{+/-}$ and Epo-Tag$^{+/+}$ littermates. Because OP waveforms (excluding OP 1, which was not analyzed in the present study) are predominantly derived from inner retinal synaptic activity,[47] the reduced amplitudes demonstrate specific impairment of inner retinal function in OIR. However, no differences in OP characteristics were detected between Epo-Tag$^{+/-}$ and Epo-Tag$^{+/+}$ littermates (Figure 5, F and G), providing further evidence that the adverse

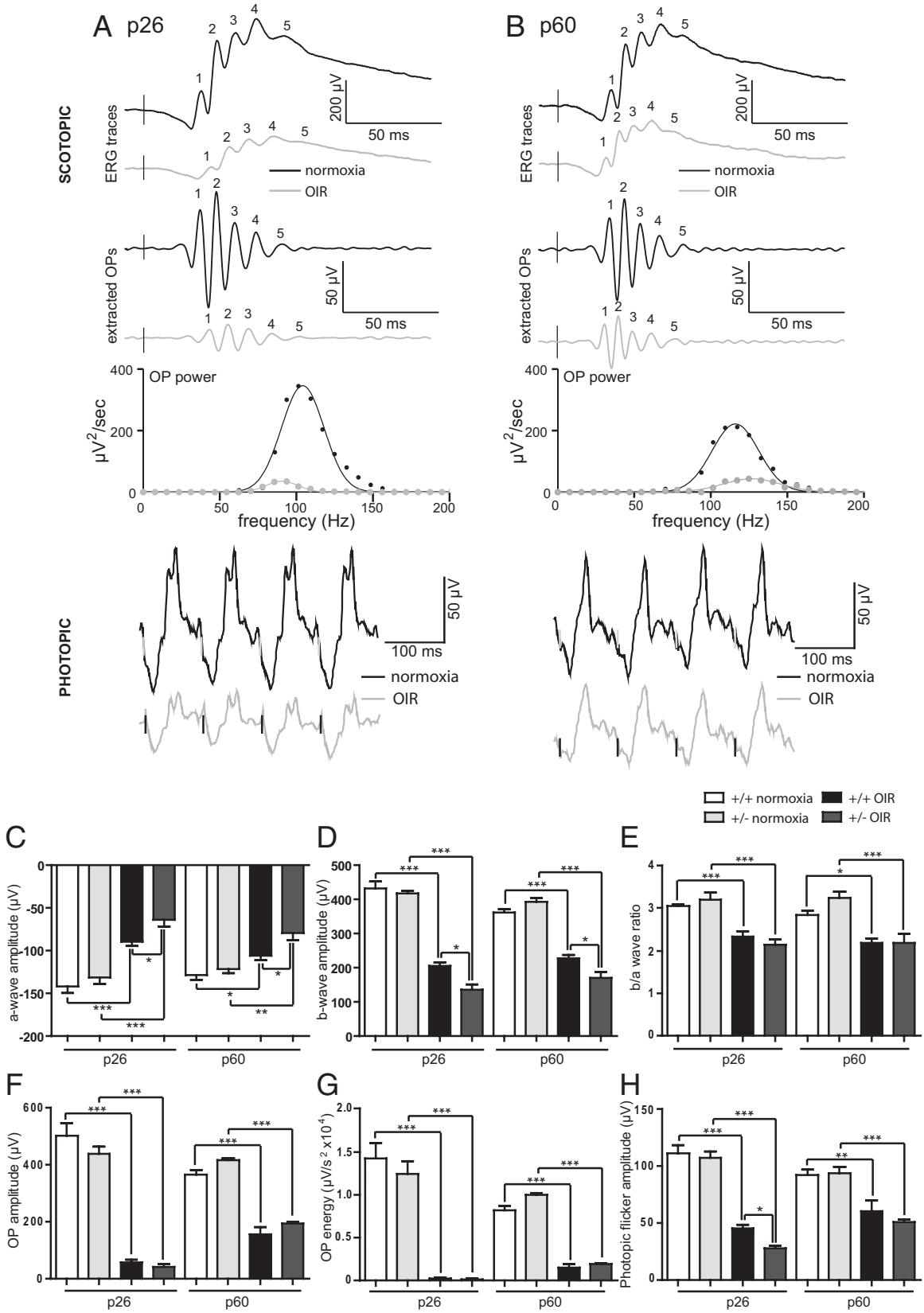

Figure 5. OIR is related to sustained inhibition of scotopic and photopic retinal function, EPO deficiency exacerbates retinal dysfunction. **A** and **B:** Representative scotopic flash traces (0.1 cd · s/m^2), extracted scotopic OPs, OP power graphs, and photopic flicker traces are shown (10 Hz), taken from normoxic and OIR Epo-Tag$^{+/+}$ animals at p26 (**A**) and p60 (**B**). OIR resulted in sustained inhibition of scotopic a-wave (**C**), b-wave (**D**), b/a wave ratio (**E**), OP sum of peak amplitude (**F**), OP energy (**G**), and photopic flicker amplitude (**H**). $n = 6$, Epo-Tag$^{+/+}$ normoxia; $n = 4$, Epo-Tag$^{+/-}$ normoxia; $n = 9$, Epo-Tag$^{+/+}$ OIR; $n = 7$, Epo-Tag$^{+/-}$ OIR. $^{*}P < 0.05$, $^{**}P < 0.01$, and $^{***}P < 0.001$ two-way analysis of variance with Bonferroni post hoc test.

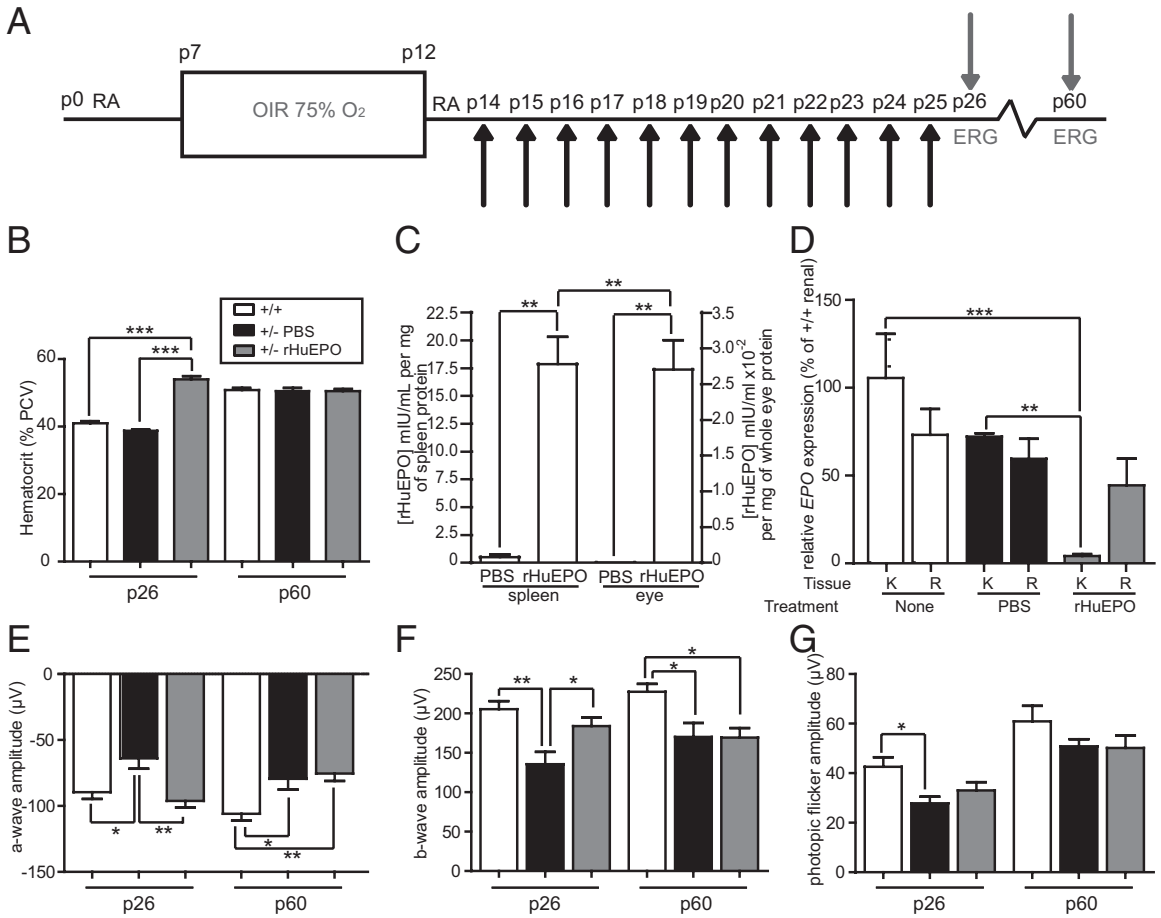

Figure 6. Systemic rHuEPO supplementation transiently corrects the retinal dysfunction associated with EPO deficiency in Epo-Tag$^{+/-}$ mice with OIR. **A:** Epo-Tag$^{+/-}$ mice were treated with rHuEPO as outlined. **Black arrows** indicate dosing with rHuEPO; **gray arrows** indicate samples collected for examination. **B:** rHuEPO supplementation was associated with an increase in hematocrit (%PCV) at p26 that was corrected by p60 (n = 3 per group at p26; n = 6 per group at p60). **C:** Small but significant amounts of rHuEPO were detected in the spleen and eye 4 hours after supplementation; significantly more was detected in the spleen than the eye (n = 3 per group). Note separate scales on the y axis for eye and spleen concentrations. **D:** rHuEPO supplementation caused suppression of endogenous *EPO* expression in the kidney, but not in the retina (n = 3 per group). **E** to **G:** rHuEPO supplementation rescued the specific dysfunction related to EPO deficiency in Epo-Tag mice, specifically related to scotopic a-wave amplitude (**E**), b-wave amplitude (**F**), and photopic flicker amplitude (**G**) (n = 10, Epo-Tag$^{+/+}$ no injection; n = 7, Epo-Tag$^{+/-}$ PBS injection; n = 8, Epo-Tag$^{+/-}$ rHuEPO injection). $^{*}P < 0.05$, $^{**}P < 0.01$, and $^{***}P < 0.001$ one-way analysis of variance with Bonferroni post hoc test (except unpaired t-test for panel **C**). ERG, electroretinogram; HET, heterozygous (Epo-Tag$^{+/-}$); OIR, oxygen-induced retinopathy; RA, room air; WT, wild type (Epo-Tag$^{+/+}$).

effect of EPO deficiency in OIR could be a consequence of outer retinal dysfunction.

Evaluation of photopic flicker ERGs showed that amplitudes were significantly reduced in animals with OIR at both p26 and p60 (Figure 5H), suggesting a significant effect of hypoxia on cone photoreceptor function. At p26, Epo-Tag$^{+/-}$ animals had significantly lower photopic flicker amplitudes than Epo-Tag$^{+/+}$ littermates, although by p60 this difference was not statistically significant.

Systemic EPO Replacement Rescues Retinal Dysfunction Associated with EPO Deficiency

To determine whether retinal dysfunction at p26 in Epo-Tag$^{+/-}$ mice is a consequence of EPO deficiency, we investigated whether retinal function is protected by systemic delivery of recombinant EPO. We measured the effect of OIR on Epo-Tag$^{+/-}$ mice treated with rHuEPO from p14 to p25 (Figure 6A), compared with littermate Epo-Tag$^{+/-}$ mice given PBS only and with untreated Epo-Tag$^{+/+}$ animals.

First, we determined the effect of EPO supplementation on hematocrit by measuring the %PCV at p26 (during dosing) and at p60 (35 days after the most recent dose) (n = 3 per group). At p26, administration of rHuEPO resulted in a significant increase in hematocrit (Figure 6B). At p60, the effect of rHuEPO on hematocrit was no longer apparent (n = 6 per group; Figure 6B).

To determine the amount of rHuEPO reaching the eye after intraperitoneal delivery, we measured the ocular concentration of rHuEPO by ELISA of eyes from animals at p26 (n = 3 per group; Figure 6C), 4 hours after intraperitoneal injection of either PBS or rHuEPO. We detected small amounts of rHuEPO in eyes from animals injected with rHuEPO (0.027 ± 0.007 mIU/mL rHuEPO per milligram of protein). No rHuEPO was detected in eyes from animals injected with PBS. In the same animals, the concentrations of rHuEPO were significantly higher in the spleen (17.85 ±

4.272 mIU/mL rHuEPO per milligram of protein) than in the eye, and were significantly higher compared with PBS-treated animals (0.52 ± 0.2 mIU/mL rHuEPO per milligram of protein) (Figure 6C). These data indicate that systemically delivered (intraperitoneal) rHuEPO achieves lower concentrations in the eye than in the spleen.

To investigate the effect of rHuEPO supplementation on local production of *EPO* in the tissue, we performed real-time RT-PCR for *mEPO* on retinas and kidneys from Epo-Tag$^{+/+}$ animals and PBS or rHuEPO treated Epo-Tag$^{+/-}$ animals at p26 (24 hours after injection). Intraperitoneal injection of rHuEPO in Epo-Tag$^{+/-}$ mice resulted in significant suppression of renal EPO expression, but no measureable suppression of retinal EPO expression (Figure 6D). These data suggest that systemically delivered EPO has a negative feedback effect on local production of *EPO* in the kidney, but not in the eye.

To determine the effect of systemic rHuEPO administration on retinal function, we performed ERGs at p26 and p60 (n = 10, Epo-Tag$^{+/+}$ untreated; n = 7, Epo-Tag$^{+/-}$ PBS-treated; n = 8, Epo-Tag$^{+/-}$ rHuEPO treated). Intraperitoneal administration of rHuEPO rescued the reduced a-wave amplitude in Epo-Tag$^{+/-}$ mice with OIR at p26 to a level similar to that of wild-type animals with OIR (Figure 6E) and also led to a proportional rescue of the b-wave amplitudes (Figure 6F); however, these effects were not sustained beyond the period of rHuEPO administration at p60 (Figure 6, E and F). Photopic flicker amplitudes were unaffected by rHuEPO treatment in Epo-Tag$^{+/-}$, compared with PBS-treated littermates at p26 or p60 (Figure 6G). Body weight did not differ significantly between groups at p26 (data not shown). Overall, these data suggest that the transient rescue effect of systemic EPO in Epo-Tag$^{+/-}$ mice correlates well with the changes observed in the systemic hematocrit levels. These data also indicate that the retinal dysfunction in Epo-Tag$^{+/-}$ mice can be attributed directly to EPO deficiency, and not to a toxic effect of the SV40T insertion.

To investigate whether systemic supplementation with EPO in non-EPO-deficient animals can rescue the neuroretinal dysfunction induced by OIR, we administered rHuEPO systemically to Epo-Tag$^{+/+}$ animals with OIR from p14 to p25, but found no evidence of any rescue of the ERG abnormalities (see Supplemental Figure S2 at *http://ajp.amjpathol.org*).

Discussion

With the present study, we have identified and quantitatively measured the neuroretinal consequences of OIR in terms of both retinal dysfunction and degeneration. We have demonstrated that OIR in the mouse induces both neuroretinal degeneration and sustained retinal dysfunction that affects predominantly the inner retina. OIR is associated with up-regulated expression of endogenous *EPO* in both the retina and kidney at p13, and with a reduction in hematocrit. We investigated the role of EPO in ischemia-induced retinopathy using EPO-deficient Epo-Tag$^{+/-}$ transgenic mice. We found that EPO deficiency in these animals did not affect the vascular response to OIR or exacerbate the inner retinal degeneration, but resulted in exaggerated neuroretinal dysfunction affecting predominantly the outer retina (as demonstrated by reduced scotopic a- and b-wave amplitudes and photopic flicker amplitudes). This dysfunction could be rescued by systemic administration of rHuEPO. We conclude that endogenous EPO protects against retinal dysfunction in OIR by increasing oxygen delivery to the eye, but found no evidence that systemic supplementation in EPO-competent mice provides additional beneficial effects.

Retinal ischemia in OIR is associated with the induction of apoptosis (which is most pronounced in cells of the inner nuclear layer) and is associated with retinal ischemia/hypoxia both spatially and temporally. Although exposure to hyperoxia can induce retinal apoptosis directly,[52–55] the absence of significant apoptosis in any retinal layer immediately after the 5 days of hyperoxia (at p12 + 0 hours) and the onset of apoptosis shortly after withdrawal from hyperoxia suggest that the cell death is the result of ischemia/hypoxia and not hyperoxia. In other models of vascular occlusion, retinal ischemia results in high levels of inner retinal apoptosis within 24 hours.[10,56] We have found that the peak of apoptosis in OIR occurs before p17, although retinal ischemia is evident also after this stage.[13]

Apoptosis of cells in the inner retina during ischemia/hypoxia in OIR is associated with thinning of the inner nuclear layer, nerve fiber layer, and inner and outer plexiform layers in the central retina. This is consistent with reports that insufficiency of the superficial and deep retinal vascular plexus results in degeneration of the inner and outer plexiform layers, respectively.[57,58] The distribution of degeneration of the inner retina in OIR is restricted to the central retina, consistent with a direct effect of ischemia/hypoxia in this area. The supply of oxygen to the plexiform layers in the developing eye is limited by incomplete vascular development, and even in adult animals the oxygen tension in these layers of the retina is relatively low.[59,60] OIR results in delayed development of the deep vascular plexus,[61] which could contribute to hypoxia-induced degeneration of the outer plexiform layer.

Previous studies have demonstrated that EPO can protect the retina against ischemic injury[38] and against light-induced retinal degeneration.[26,39] Others have described dose-dependent antiapoptotic and neuroprotective effects of intraocular EPO administration.[41,62] In the present study, ischemia-induced degeneration of the inner retina was not exacerbated by endogenous EPO deficiency in Epo-Tag$^{+/-}$ mice with OIR. This finding does not, however, exclude a neuroprotective effect of EPO in OIR, because the EPO deficiency in these animals is incomplete. Although Epo-Tag$^{+/-}$ mice are deficient in EPO, they are nonetheless able to maintain low-level EPO expression and demonstrate up-regulated *EPO* expression in response to hypoxia.

In animals with OIR, we detected an increased frequency of apoptosis in cells in the outer nuclear layer (which comprises nuclei of photoreceptor cells) within 24 hours of the onset of retinal hypoxia/ischemia. Only a

small proportion of the cells were apoptotic, and we did not detect any associated effect on outer nuclear layer thickness at p60. The outer nuclear layer depends for its function and survival on normal perfusion of the choroidal circulation.[60] The mechanism of photoreceptor apoptosis during retinal ischemia in OIR is not clear, but may be a consequence of choroidal degeneration[63] or of slightly reduced hematocrit leading to photoreceptor hypoxia, apoptosis, and corresponding functional deficits.[63]

We identified sustained neuroretinal dysfunction in murine OIR, as demonstrated by reduced scotopic and photopic ERG responses. Substantial reductions in ERG b-wave amplitudes, b/a wave ratio, and OPs indicating inner retinal disease are consistent with dysfunction and degeneration associated with retinal ischemia. The reduced amplitude of OPs in murine OIR is consistent with changes previously reported in rat OIR.[8] In addition, we detected a reduction in ERG a-wave, indicating dysfunction of photoreceptor cells. An effect on light-adapted ERG responses indicates a negative effect on the function of cone photoreceptors. OIR is generally considered to be a disorder of the retinal vasculature, and an effect on photoreceptor function in mice has not previously been described. Future studies could use the techniques presented here to investigate neuroprotective agents or to evaluate potential neuronal adverse effects of antiangiogenic treatments.

We detected no retinal dysfunction in Epo-Tag$^{+/-}$ mice reared in normoxia, suggesting that normal EPO expression is not critical for retinal function in normal conditions. However, EPO deficiency in Epo-Tag$^{+/-}$ mice was associated with a significantly more pronounced effect on ERG a-wave and b-wave amplitudes in OIR. The lack of a significant difference in b/a wave ratio or additional OP abnormalities suggests that the particular vulnerability of EPO deficiency in OIR can be attributed predominantly to dysfunction of the outer retina. Cone photoreceptor responses were significantly reduced in Epo-Tag$^{+/-}$ mice at p26, but showed significant recovery by p60, indicating that the insult that leads to a reduction in cone function is temporary, allowing the cones to recover by day 60.

The EPO deficiency in Epo-Tag$^{+/-}$ mice was not associated with a significant effect on the typical retinal vascular response to OIR. These animals developed a slightly larger area of retinal ischemia after exposure to oxygen, but demonstrated a typical neovascular response to hypoxia by p17. There is considerable variability in the proangiogenic activity of EPO, which is contextual and depends on the species,[62,64] the stage of OIR,[17,18,33] and the EPO subtype.[65] Differences in the effects of EPO supplementation on retinal vasculature between these reports and the present findings may reflect differences in the nature of the EPO preparation, in the dose, timing, and route of delivery, and in the models used. In the present study, EPO deficiency in Epo-Tag$^{+/-}$ mice in OIR was incomplete, and residual EPO activity may be sufficient to induce appropriate angiogenesis in this context or to facilitate the activity of other potent angiogenic factors inducing neovascularization (such as VEGF).[66] The effects of EPO are also dependent on the site of EPO receptor (EPO-R) expression. Previous studies have identified EPO-R expression in retinal ganglion cells,[67] Müller glia,[68] and retinal photoreceptors.[26,39] The nature of the retinal disease process may affect the location and extent of EPO-R expression.[28,69] The distribution of EPO-R expression in mouse OIR, however, has yet to be described.

The protection of Epo-Tag$^{+/-}$ mice against retinal dysfunction in OIR by systemic rHuEPO supplementation was associated with an increase in hematocrit. rHuEPO administered systemically could be detected at very low concentrations in the eye, compared with the spleen, and significantly suppressed renal but not retinal expression of endogenous *EPO*. These data indicate that the additional outer retinal dysfunction apparent in EPO-deficient Epo-Tag$^{+/-}$ mice with OIR may be a result of impaired oxygen delivery to the outer retina. Outer retinal dysfunction occurs secondary to systemic hypoxia, with sparing of the inner retina through compensatory autoregulation of blood flow within the inner retinal circulation.[70] Systemic but not intraocular EPO supplementation protects retinal photoreceptor cells against light-induced damage and against certain hereditary retinal degenerations.[71] Another role for EPO in neuroprotection might be its inhibitory effect on microglial activation. EPO deficiency would be expected to contribute further to the enhanced microglial activation seen in mouse OIR.[72] These effects could directly affect microglial phagocytic activity, or indirectly affect release of proinflammatory cytokines, although recent studies in the brain suggest that cytokine effects of EPO are less significant than those on microglial proliferation.[73] Microglial activation can protect against photoreceptor degeneration,[74] and it is conceivable that the effect of EPO deficiency on increased retinal microglial activity may have contributed to the enhanced photoreceptor dysfunction that we observed.

In the present study, EPO deficiency in Epo-Tag$^{+/-}$ mice was compatible with normal retinal function in normoxia as measured by electroretinography, but it exacerbated ischemic injury in OIR. Dysfunction of the outer retina may reflect impaired oxygen delivery secondary to anemia in Epo-Tag EPO-deficient mice with OIR, given the uniquely high demand of photoreceptor cells for oxygen. The present findings raise the possibility that systemic rHuEPO supplementation therapy for anemia of prematurity might protect outer retinal function against ischemic injury in retinopathy of prematurity without exacerbating the development of pathological neovascularization.[75]

Acknowledgments

We thank Edward Lee for assistance with cone flicker ERGs, Susie Barker for ELISA assistance, and Nicky Gent and the University College London Biological Resource Unit staff for assistance with animal management.

References

1. Bek T: Inner retinal ischaemia: current understanding and needs for further investigations. Acta Ophthalmol 2009, 87:362–367

2. Wittström E, Ponjavic V, Lövestam-Adrian M, Larsson J, Andréasson S: Electrophysiological evaluation and visual outcome in patients with central retinal vein occlusion, primary open-angle glaucoma and neovascular glaucoma. Acta Ophthalmol 2010, 88:86–90
3. Rehak J, Rehak M: Branch retinal vein occlusion: pathogenesis, visual prognosis, and treatment modalities. Curr Eye Res 2008, 33: 111–131
4. Sapieha P, Joyal JS, Rivera JC, Kermorvant-Duchemin E, Sennlaub F, Hardy P, Lachapelle P, Chemtob S: Retinopathy of prematurity: understanding ischemic retinal vasculopathies at an extreme of life. J Clin Invest 2010, 120:3022–3032
5. Rosenbaum DM, Rosenbaum PS, Gupta A, Michaelson MD, Hall DH, Kessler JA: Retinal ischemia leads to apoptosis which is ameliorated by aurintricarboxylic acid. Vision Res 1997, 37:3445–3451
6. Fulton AB, Hansen RM, Petersen RA, Vanderveen DK: The rod photoreceptors in retinopathy of prematurity: an electroretinographic study. Arch Ophthalmol 2001, 119:499–505
7. Fulton AB, Hansen RM: Electroretinogram responses and refractive errors in patients with a history of retinopathy prematurity. Doc Ophthalmol 1995, 91:87–100
8. Akula JD, Mocko JA, Moskowitz A, Hansen RM, Fulton AB: The oscillatory potentials of the dark-adapted electroretinogram in retinopathy of prematurity. Invest Ophthalmol Vis Sci 2007, 48:5788–5797
9. Osborne NN, Casson RJ, Wood JP, Chidlow G, Graham M, Melena J: Retinal ischemia: mechanisms of damage and potential therapeutic strategies. Prog Retin Eye Res 2004, 23:91–147
10. Dijk F, Bergen AA, Kamphuis W: GAP-43 expression is upregulated in retinal ganglion cells after ischemia/reperfusion-induced damage. Exp Eye Res 2007, 84:858–867
11. Aizu Y, Oyanagi K, Hu J, Nakagawa H: Degeneration of retinal neuronal processes and pigment epithelium in the early stage of the streptozotocin-diabetic rats. Neuropathology 2002, 22:161–170
12. Gastinger MJ, Singh RS, Barber AJ: Loss of cholinergic and dopaminergic amacrine cells in streptozotocin-diabetic rat and Ins2Akita-diabetic mouse retinas. Invest Ophthalmol Vis Sci 2006, 47:3143–3150
13. Smith LE, Wesolowski E, McLellan A, Kostyk SK, D'Amato R, Sullivan R, D'Amore PA: Oxygen-induced retinopathy in the mouse. Invest Ophthalmol Vis Sci 1994, 35:101–111
14. Ozaki H, Seo MS, Ozaki K, Yamada H, Yamada E, Okamoto N, Hofmann F, Wood JM, Campochiaro PA: Blockade of vascular endothelial cell growth factor receptor signaling is sufficient to completely prevent retinal neovascularization. Am J Pathol 2000, 156:697–707
15. Pechan P, Rubin H, Lukason M, Ardinger J, DuFresne E, Hauswirth WW, Wadsworth SC, Scaria A: Novel anti-VEGF chimeric molecules delivered by AAV vectors for inhibition of retinal neovascularization. Gene Ther 2009, 16:10–16
16. Konopatskaya O, Churchill AJ, Harper SJ, Bates DO, Gardiner TA: VEGF165b, an endogenous C-terminal splice variant of VEGF, inhibits retinal neovascularization in mice. Mol Vis 2006, 12:626–632
17. Watanabe D, Suzuma K, Matsui S, Kurimoto M, Kiryu J, Kita M, Suzuma I, Ohashi H, Ojima T, Murakami T, Kobayashi T, Masuda S, Nagao M, Yoshimura N, Takagi H: Erythropoietin as a retinal angiogenic factor in proliferative diabetic retinopathy. N Engl J Med 2005, 353:782–792
18. Chen J, Connor KM, Aderman CM, Willett KL, Aspegren OP, Smith LE: Suppression of retinal neovascularization by erythropoietin siRNA in a mouse model of proliferative retinopathy. Invest Ophthalmol Vis Sci 2009, 50:1329–1335
19. Xiong SQ, Xia XB, Xu HZ, Jiang J: Suppression of retinal neovascularization by small-interference RNA targeting erythropoietin. Ophthalmologica 2009, 223:306–312
20. Akula JD, Hansen RM, Martinez-Perez ME, Fulton AB: Rod photoreceptor function predicts blood vessel abnormality in retinopathy of prematurity. Invest Ophthalmol Vis Sci 2007, 48:4351–4359
21. Akula JD, Mocko JA, Benador IY, Hansen RM, Favazza TL, Vyhovsky TC, Fulton AB: The neurovascular relation in oxygen-induced retinopathy. Mol Vis 2008, 14:2499–2508
22. Reynaud X, Hansen RM, Fulton AB: Effect of prior oxygen exposure on the electroretinographic responses of infant rats. Invest Ophthalmol Vis Sci 1995, 36:2071–2079
23. Eckardt KU, Ratcliffe PJ, Tan CC, Bauer C, Kurtz A: Age-dependent expression of the erythropoietin gene in rat liver and kidneys. J Clin Invest 1992, 89:753–760
24. Yu X, Shacka JJ, Eells JB, Suarez-Quian C, Przygodzki RM, Beleslin-Cokic B, Lin CS, Nikodem VM, Hempstead B, Flanders KC, Costantini F, Noguchi CT: Erythropoietin receptor signalling is required for normal brain development. Development 2002, 129:505–516
25. Chavez JC, Baranova O, Lin J, Pichiule P: The transcriptional activator hypoxia inducible factor 2 (HIF-2/EPAS-1) regulates the oxygen-dependent expression of erythropoietin in cortical astrocytes. J Neurosci 2006, 26:9471–9481
26. Grimm C, Wenzel A, Groszer M, Mayser H, Seeliger M, Samardzija M, Bauer C, Gassmann M, Reme CE: HIF-1-induced erythropoietin in the hypoxic retina protects against light-induced retinal degeneration. Nat Med 2002, 8:718–724
27. Morita M, Ohneda O, Yamashita T, Takahashi S, Suzuki N, Nakajima O, Kawauchi S, Ema M, Shibahara S, Udono T, Tomita K, Tamai M, Sogawa K, Yamamoto M, Fujii-Kuriyama Y: HLF/HIF-2alpha is a key factor in retinopathy of prematurity in association with erythropoietin. EMBO J 2003, 22:1134–1146
28. Shah SS, Tsang SH, Mahajan VB: Erythropoetin receptor expression in the human diabetic retina. BMC Res Notes 2009, 2:234
29. Stahl A, Buchwald A, Martin G, Junker B, Chen J, Hansen LL, Agostini HT, Smith LE, Feltgen N: Vitreal levels of erythropoietin are increased in patients with retinal vein occlusion and correlate with vitreal VEGF and the extent of macular edema. Retina 2010, 30:1524–1529
30. Inomata Y, Hirata A, Takahashi E, Kawaji T, Fukushima M, Tanihara H: Elevated erythropoietin in vitreous with ischemic retinal diseases. Neuroreport 2004, 15:877–879
31. Katsura Y, Okano T, Matsuno K, Osako M, Kure M, Watanabe T, Iwaki Y, Noritake M, Kosano H, Nishigori H, Matsuoka T: Erythropoietin is highly elevated in vitreous fluid of patients with proliferative diabetic retinopathy. Diabetes Care 2005, 28:2252–2254
32. Sato T, Kusaka S, Shimojo H, Fujikado T: Vitreous levels of erythropoietin and vascular endothelial growth factor in eyes with retinopathy of prematurity. Ophthalmology 2009, 116:1599–1603
33. Chen J, Connor KM, Aderman CM, Smith LE: Erythropoietin deficiency decreases vascular stability in mice. J Clin Invest 2008, 118: 526–533
34. Suk KK, Dunbar JA, Liu A, Daher NS, Leng CK, Leng JK, Lim P, Weller S, Fayard E: Human recombinant erythropoietin and the incidence of retinopathy of prematurity: a multiple regression model. J AAPOS 2008, 12:233–238
35. Saint-Geniez M, Maharaj AS, Walshe TE, Tucker BA, Sekiyama E, Kurihara T, Darland DC, Young MJ, D'Amore PA: Endogenous VEGF is required for visual function: evidence for a survival role on muller cells and photoreceptors. PLoS One 2008, 3:e3554
36. Nishijima K, Ng YS, Zhong L, Bradley J, Schubert W, Jo N, Akita J, Samuelsson SJ, Robinson GS, Adamis AP, Shima DT: Vascular endothelial growth factor-A is a survival factor for retinal neurons and a critical neuroprotectant during the adaptive response to ischemic injury. Am J Pathol 2007, 171:53–67
37. Brines ML, Ghezzi P, Keenan S, Agnello D, de Lanerolle NC, Cerami C, Itri LM, Cerami A: Erythropoietin crosses the blood-brain barrier to protect against experimental brain injury. Proc Natl Acad Sci USA 2000, 97:10526–10531
38. Junk AK, Mammis A, Savitz SI, Singh M, Roth S, Malhotra S, Rosenbaum PS, Cerami A, Brines M, Rosenbaum DM: Erythropoietin administration protects retinal neurons from acute ischemia-reperfusion injury. Proc Natl Acad Sci USA 2002, 99:10659–10664
39. Grimm C, Wenzel A, Stanescu D, Samardzija M, Hotop S, Groszer M, Naash M, Gassmann M, Remé C: Constitutive overexpression of human erythropoietin protects the mouse retina against induced but not inherited retinal degeneration. J Neurosci 2004, 24:5651–5658
40. Grimm C, Hermann DM, Bogdanova A, Hotop S, Kilic U, Wenzel A, Kilic E, Gassmann M: Neuroprotection by hypoxic preconditioning: HIF-1 and erythropoietin protect from retinal degeneration. Semin Cell Dev Biol 2005, 16:531–538
41. Weishaupt JH, Rohde G, Pölking E, Siren AL, Ehrenreich H, Bähr M: Effect of erythropoietin axotomy-induced apoptosis in rat retinal ganglion cells. Invest Ophthalmol Vis Sci 2004, 45:1514–1522
42. Bierer R, Peceny MC, Hartenberger CH, Ohls RK: Erythropoietin concentrations and neurodevelopmental outcome in preterm infants. Pediatrics 2006, 118:e635–e640

43. Brown MS, Eichorst D, Lala-Black B, Gonzalez R: Higher cumulative doses of erythropoietin and developmental outcomes in preterm infants. Pediatrics 2009, 124:e681–e687
44. Maxwell PH, Osmond MK, Pugh CW, Heryet A, Nicholls LG, Tan CC, Doe BG, Ferguson DJ, Johnson MH, Ratcliffe PJ: Identification of the renal erythropoietin-producing cells using transgenic mice. Kidney Int 1993, 44:1149–1162
45. Raja KB, Maxwell PH, Ratcliffe PJ, Salisbury JR, Simpson RJ, Peters TJ: Iron metabolism in transgenic mice with hypoplastic anaemia due to incomplete deficiency of erythropoietin. Br J Haematol 1997, 96: 248–253
46. Lei B, Yao G, Zhang K, Hofeldt KJ, Chang B: Study of rod- and cone-driven oscillatory potentials in mice. Invest Ophthalmol Vis Sci 2006, 47:2732–2738
47. Krishna VR, Alexander KR, Peachey NS: Temporal properties of the mouse cone electroretinogram. J Neurophysiol 2002, 87:42–48
48. Gardiner TA, Gibson DS, de Gooyer TE, de la Cruz VF, McDonald DM, Stitt AW: Inhibition of tumor necrosis factor-alpha improves physiological angiogenesis and reduces pathological neovascularization in ischemic retinopathy. Am J Pathol 2005, 166:637–644
49. Banin E, Dorrell MI, Aguilar E, Ritter MR, Aderman CM, Smith AC, Friedlander J, Friedlander M: T2-TrpRS inhibits preretinal neovascularization and enhances physiological vascular regrowth in OIR as assessed by a new method of quantification. Invest Ophthalmol Vis Sci 2006, 47:2125–2134
50. Mowat FM, Luhmann UF, Smith AJ, Lange C, Duran Y, Harten S, Shukla D, Maxwell PH, Ali RR, Bainbridge JW: HIF-1alpha and HIF-2alpha are differentially activated in distinct cell populations in retinal ischaemia. PLoS One 2010, 5:e11103
51. Shinoda K, Yamada K, Matsumoto CS, Kimoto K, Nakatsuka K: Changes in retinal thickness are correlated with alterations of electroretinogram in eyes with central retinal artery occlusion. Graefes Arch Clin Exp Ophthalmol 2008, 246:949–954
52. Natoli R, Provis J, Valter K, Stone J: Expression and role of the early-response gene Oxr1 in the hyperoxia-challenged mouse retina. Invest Ophthalmol Vis Sci 2008, 49:4561–4567
53. Yamada H, Yamada E, Ando A, Esumi N, Bora N, Saikia J, Sung CH, Zack DJ, Campochiaro PA: Fibroblast growth factor-2 decreases hyperoxia-induced photoreceptor cell death in mice. Am J Pathol 2001, 159:1113–1120
54. Walsh N, Bravo-Nuevo A, Geller S, Stone J: Resistance of photoreceptors in the C57BL/6-c2J, C57BL/6J, and BALB/cJ mouse strains to oxygen stress: evidence of an oxygen phenotype. Curr Eye Res 2004, 29:441–447
55. Wellard J, Lee D, Valter K, Stone J: Photoreceptors in the rat retina are specifically vulnerable to both hypoxia and hyperoxia. Vis Neurosci 2005, 22:501–507
56. Rosenbaum DM, Rosenbaum PS, Gupta H, Singh M, Aggarwal A, Hall DH, Roth S, Kessler JA: The role of the p53 protein in the selective vulnerability of the inner retina to transient ischemia. Invest Ophthalmol Vis Sci 1998, 39:2132–2139
57. Mayor-Torroglosa S, De la Villa P, Rodríguez ME, López-Herrera MP, Avilés-Trigueros M, García-Avilés A, de Imperial JM, Villegas-Pérez MP, Vidal-Sanz M: Ischemia results 3 months later in altered ERG, degeneration of inner layers, and deafferented tectum: neuroprotection with brimonidine. Invest Ophthalmol Vis Sci 2005, 46:3825–3835
58. Dembinska O, Rojas LM, Varma DR, Chemtob S, Lachapelle P: Graded contribution of retinal maturation to the development of oxygen-induced retinopathy in rats. Invest Ophthalmol Vis Sci 2001, 42:1111–1118
59. Yu DY, Cringle SJ: Oxygen distribution in the mouse retina. Invest Ophthalmol Vis Sci 2006, 47:1109–1112
60. Yu DY, Cringle SJ: Oxygen distribution and consumption within the retina in vascularised and avascular retinas and in animal models of retinal disease. Prog Retin Eye Res 2001, 20:175–208
61. Alon T, Hemo I, Itin A, Pe'er J, Stone J, Keshet E: Vascular endothelial growth factor acts as a survival factor for newly formed retinal vessels and has implications for retinopathy of prematurity. Nat Med 1995, 1:1024–1028
62. Zhang J, Wu Y, Jin Y, Ji F, Sinclair SH, Luo Y, Xu G, Lu L, Dai W, Yanoff M, Li W, Xu GT: Intravitreal injection of erythropoietin protects both retinal vascular and neuronal cells in early diabetes. Invest Ophthalmol Vis Sci 2008, 49:732–742
63. Shao Z, Dorfman AL, Seshadri S, Djavari M, Kermorvant-Duchemin E, Sennlaub F, Blais M, Polosa A, Varma DR, Joyal JS, Lachapelle P, Hardy P, Sitaras N, Picard E, Mancini J, Sapieha P, Chemtob S: Choroidal involution is a key component of oxygen induced retinopathy. Invest Ophthalmol Vis Sci 2011, 52:6238–6248
64. Slusarski JD, McPherson RJ, Wallace GN, Juul SE: High-dose erythropoietin does not exacerbate retinopathy of prematurity in rats. Pediatr Res 2009, 66:625–630
65. McVicar CM, Colhoun LM, Abrahams JL, Kitson CL, Hamilton R, Medina RJ, Durga D, Gardiner TA, Rudd PM, Stitt AW: Differential modulation of angiogenesis by erythropoiesis-stimulating agents in a mouse model of ischaemic retinopathy. PLoS One 2010, 5:e11870
66. Kertesz N, Wu J, Chen TH, Sucov HM, Wu H: The role of erythropoietin in regulating angiogenesis. Dev Biol 2004, 276:101–110
67. Zhong L, Bradley J, Schubert W, Ahmed E, Adamis AP, Shima DT, Robinson GS, Ng YS: Erythropoietin promotes survival of retinal ganglion cells in DBA/2J glaucoma mice. Invest Ophthalmol Vis Sci 2007, 48:1212–1218
68. Krügel K, Wurm A, Linnertz R, Pannicke T, Wiedemann P, Reichenbach A, Bringmann A: Erythropoietin inhibits osmotic swelling of retinal glial cells by Janus kinase- and extracellular signal-regulated kinases1/2-mediated release of vascular endothelial growth factor. Neuroscience 2010, 165:1147–1158
69. Dreixler JC, Hagevik S, Hemmert JW, Shaikh AR, Rosenbaum DM, Roth S: Involvement of erythropoietin in retinal ischemic preconditioning. Anesthesiology 2009, 110:774–780
70. Linsenmeier RA: Electrophysiological consequences of retinal hypoxia. Graefes Arch Clin Exp Ophthalmol 1990, 228:143–150
71. Rex TS, Allocca M, Domenici L, Surace EM, Maguire AM, Lyubarsky A, Cellerino A, Bennett J, Auricchio A: Systemic but not intraocular Epo gene transfer protects the retina from light-and genetic-induced degeneration. Mol Ther 2004, 10:855–861
72. McVicar CM, Hamilton R, Colhoun LM, Gardiner TA, Brines M, Cerami A, Stitt AW: Intervention with an erythropoietin-derived peptide protects against neuroglial and vascular degeneration during diabetic retinopathy. Diabetes 2011, 60:2995–3005
73. Wilms H, Schwabedissen B, Sievers J, Lucius R: Erythropoietin does not attenuate cytokine production and inflammation in microglia–implications for the neuroprotective effect of erythropoietin in neurological diseases. J Neuroimmunol 2009, 212:106–111
74. Sasahara M, Otani A, Oishi A, Kojima H, Yodoi Y, Kameda T, Nakamura H, Yoshimura N: Activation of bone marrow-derived microglia promotes photoreceptor survival in inherited retinal degeneration. Am J Pathol 2008, 172:1693–703
75. Schneider JK, Gardner DK, Cordero L: Use of recombinant human erythropoietin and risk of severe retinopathy in extremely low-birthweight infants. Pharmacotherapy 2008, 28:1335–1340